Electronic Supplementary Material (ESI) for Physical Chemistry Chemical Physics.

Supplementary Information

An intrinsic room-temperature half-metallic ferromagnet in metal-free PN_2 monolayer

Quan Zhang, Yang Zhang, Ying Li, Dangqi Fang, Junwei Che, Erhu Zhang, Peng Zhang, Shengli Zhang*

MOE Key Lab for Nonequilibrium Synthesis and Modulation of Condensed Matter, School of Physics, Xi'an Jiaotong University, Xi'an, 710049, China

***Corresponding Author:** zhangsl@xjtu.edu.cn

1. Stability analysis of possible H, T and T' phases.

The atomic structures of the PN_2 monolayer in the possible H, T and T' phases are displayed in Fig. S1. During the geometric optimization, the T'-PN_2 would spontaneously transform into the T-PN_2. The H-PN_2 is dynamically unstable because of the imaginary modes in the phonon dispersion (Fig. S2(b)). And the cohesive energy of the H-PN_2 (3.41 eV/eV) is smaller than T-PN_2 (4.06 eV/atom). Among them, the T-PN_2 monolayer is found to be the energetically and dynamically stable phase.

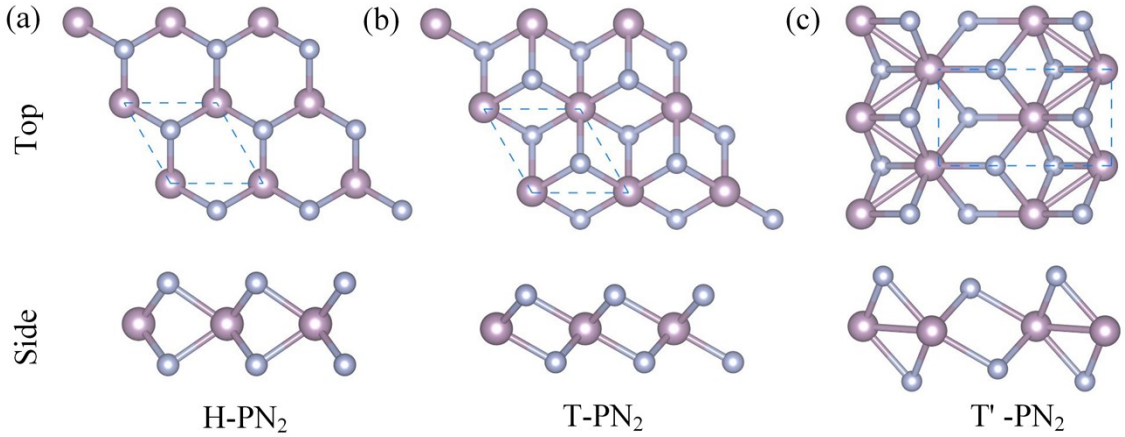

Figure S1. Atomic structures of (a) H-PN_2, (b) T-PN_2, and (c) T'-PN_2 monolayers. The dashed lines mark the primitive unit cell.

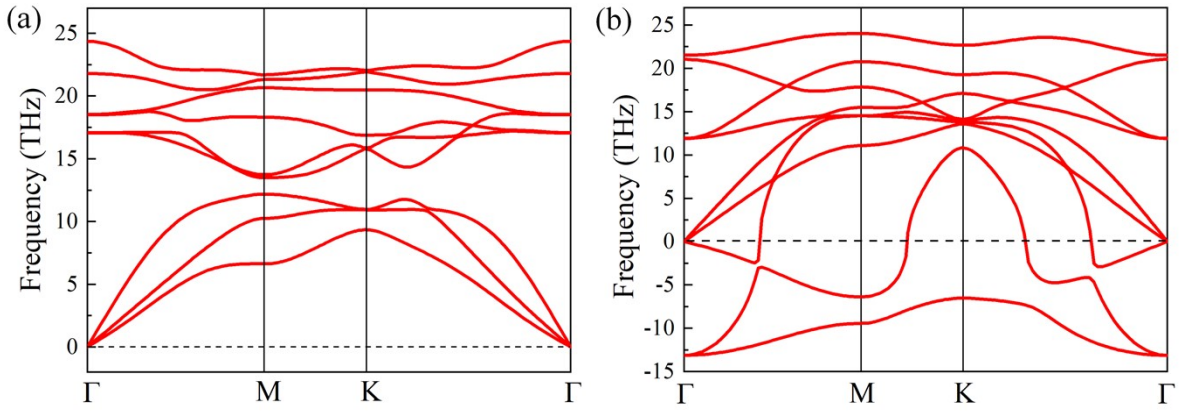

Figure S2. Phonon dispersions of (a) T-PN_2 and (b) H-PN_2 monolayers.

2. The robustness of the half-metallicity in the PN_2 monolayer.

For practical applications, the tenability of the half-metallicity is examined under an external perturbation. As shown in Figs. S3 and S4, by employing biaxial strain and carrier doping, the band structures of the PN_2 monolayer remain half-metallic characteristics i.e. the spin-down channel is metallic while the spin-up is insulating.

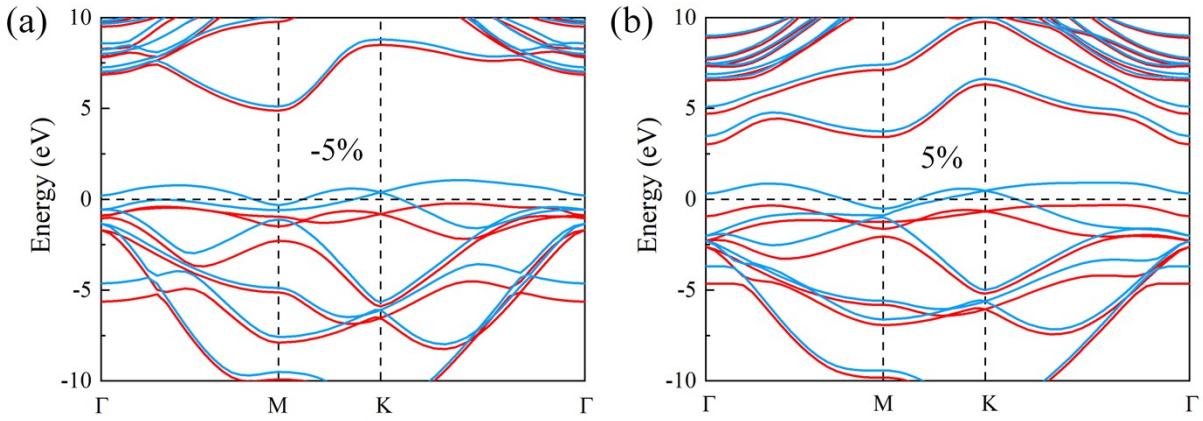

Figure S3. Band structures of the PN_2 monolayer under (a) -5% and (b) 5% biaxial strain. Red and blue colors represent the spin-up and spin-down states, respectively.

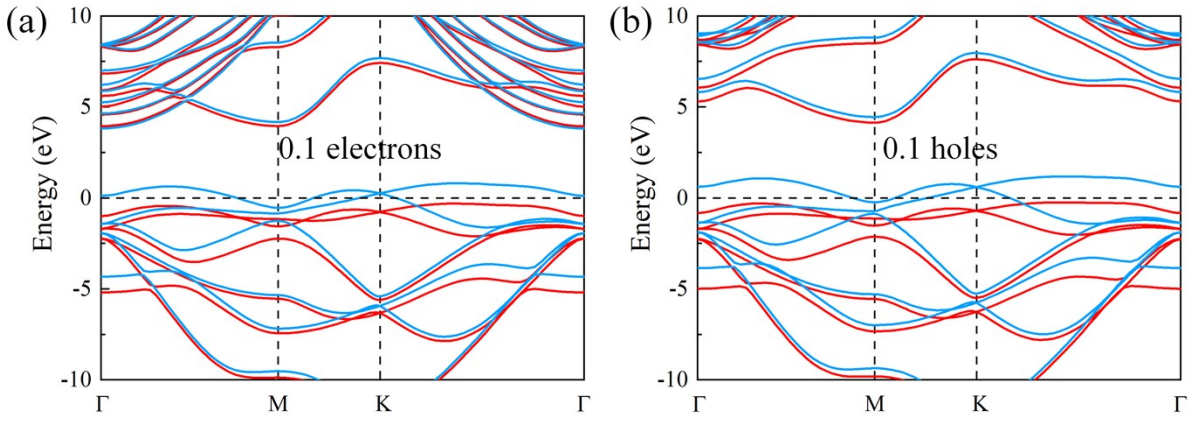

Figure S4. Band structures of the carrier doped PN_2 monolayers with carrier concentration of (a) 0.1 electrons and (b) 0.1 holes per unit cell (1.55×10^{14} cm^{-2}).

3. The effect of carrier doping on the magnetic properties of the PN_2 monolayer.

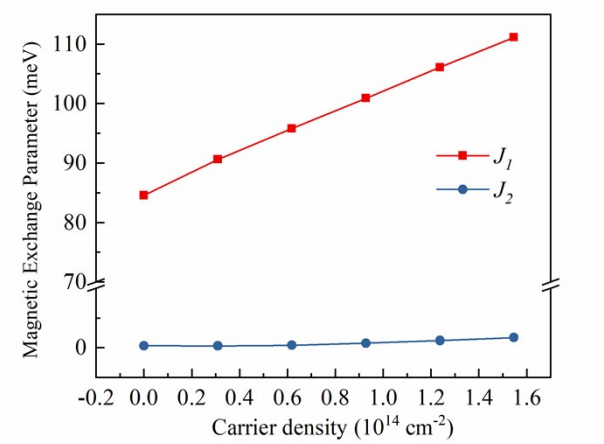

Figure S5. Magnetic exchange parameters J_1 and J_2 vary with carrier density (electron doping).

In this section, we analyze the variation of magnetic moment with carrier doping. As we well know, the magnetic moment M could be expressed by $M = N_\uparrow - N_\downarrow$, where $N_\uparrow$ and $N_\downarrow$ represent the number of electrons with spin-up and spin-down. According to the Fig. 3, when the electrons are doped, the Fermi level will shift up. Meanwhile, $N_\downarrow$ increases while $N_\uparrow$ remains unchanged, so the magnetic moment M linearly decreases. When the holes are doped under the considered ranges (0 ~ 0.1 holes per unit cell), the Fermi level will shift down. $N_\downarrow$ decreases while $N_\uparrow$ remains unchanged, so the magnetic moment M linearly increases. It should be emphasized that the doped carriers in this range are completely polarized. Thus, the variation of magnetic moment with carrier doping is linear.

Of course, when the hole doping density exceeds a certain limit (namely, when the Fermi level crosses both the spin-down and spin-up bands), both $N_\downarrow$ and $N_\uparrow$ will decrease. Because of the difference in density of states (DOS) between spin-up and spin-down, $N_\uparrow$ reduces more than $N_\downarrow$, resulting in a decrease in the magnetic moment M. At this point, the doped carriers are not completely polarized. In order to understand this phenomenon more clearly, we have investigated the effect of a larger range of hole doping on the magnetic moment. As shown in Figure S6, the magnetic moment variation trend is consistent with our previous analysis.

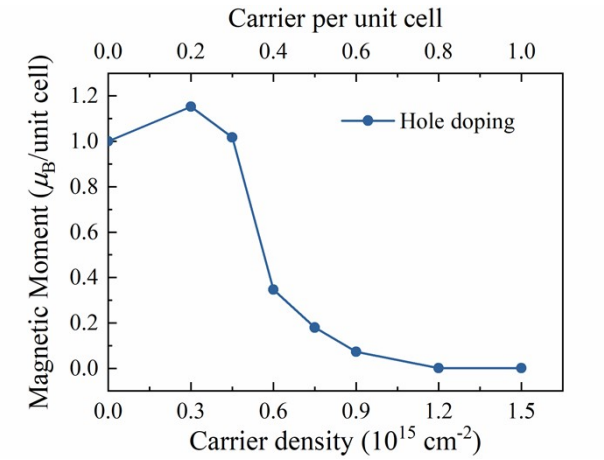

Figure S6. The carrier doping dependency of the magnetic moment of a PN_2 unit cell.